BIOCHEMISTRY
including biophysical chemistry & molecular biology

Article

pubs.acs.org/biochemistry

# Early Endosomal Escape of a Cyclic Cell-Penetrating Peptide Allows Effective Cytosolic Cargo Delivery

Ziqing Qian,[†] Jonathan R. LaRochelle,[‡] Bisheng Jiang,[†] Wenlong Lian,[†] Ryan L. Hard,[†] Nicholas G. Selner,[†] Rinrada Luechapanichkul,[†] Amy M. Barrios,[§] and Dehua Pei*[,†]

[†]Department of Chemistry and Biochemistry, The Ohio State University, 100 West 18th Avenue, Columbus, Ohio 43210, United States

[‡]Department of Molecular, Cellular, and Developmental Biology, Yale University, New Haven, Connecticut 06520-8103, United States

[§]Department of Medicinal Chemistry, University of Utah, Salt Lake City, Utah 84112, United States

Supporting Information

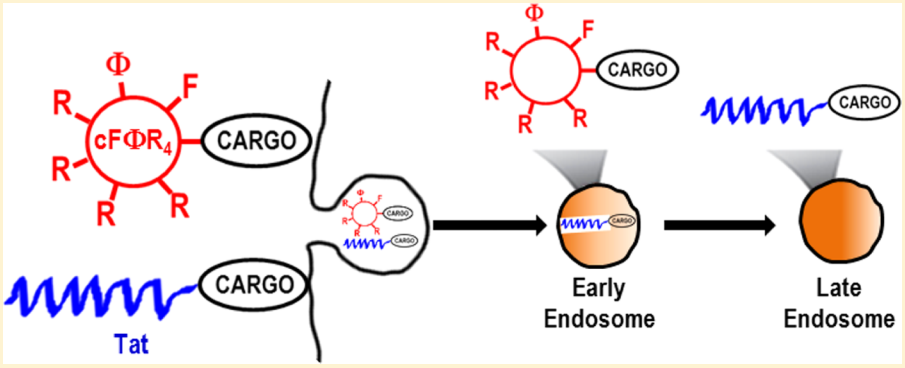


**ABSTRACT:** Cyclic heptapeptide cyclo(FΦRRRRQ) (cFΦR$_4$, where Φ is L-2-naphthylalanine) was recently found to be efficiently internalized by mammalian cells. In this study, its mechanism of internalization was investigated by perturbing various endocytic events through the introduction of pharmacologic agents and genetic mutations. The results show that cFΦR$_4$ binds directly to membrane phospholipids, is internalized into human cancer cells through endocytosis, and escapes from early endosomes into the cytoplasm. Its cargo capacity was examined with a wide variety of molecules, including small-molecule dyes, linear and cyclic peptides of various charged states, and proteins. Depending on the nature of the cargos, they may be delivered by endocyclic (insertion of cargo into the cFΦR$_4$ ring), exocyclic (attachment of cargo to the Gln side chain), or bicyclic approaches (fusion of cFΦR$_4$ and cyclic cargo rings). The overall delivery efficiency (i.e., delivery of cargo into the cytoplasm and nucleus) of cFΦR$_4$ was 4−12-fold higher than those of nonaarginine, HIV Tat-derived peptide, or penetratin. The higher delivery efficiency, coupled with superior serum stability, minimal toxicity, and synthetic accessibility, renders cFΦR$_4$ a useful transporter for intracellular cargo delivery and a suitable system for investigating the mechanism of endosomal escape.

The plasma membrane presents a major challenge in drug discovery, especially for biologics such as peptides, proteins, and nucleic acids. One potential strategy for subverting the membrane barrier and delivering the biologics into cells is to attach them to "cell-penetrating peptides" (CPPs). Since the initial observation that HIV *trans*-activator of transcription, Tat, internalizes into mammalian cells and activates viral replication in the late 1980s,[1,2] a large number of CPPs consisting of 6−20 residues have been reported.[3−8] CPPs have been used to deliver small-molecule drugs,[9,10] DNA,[11,12] RNA,[13−16] proteins,[17−19] and nanoparticles[20−22] into mammalian cells and tissues through either covalent attachment or electrostatic association. Many CPPs display minimal toxicity and immunogenicity at physiologically relevant concentrations,[23,24] and the incorporation of specific unnatural amino acids[25] and other chemical moieties[26,27] has been found to increase the stability and extent of cytosolic delivery.

Despite three decades of investigation, the fundamental basis for CPP activity remains elusive. Two distinct and non-mutually exclusive mechanisms have been proposed for the CPPs whose primary sequences are characterized by multiple arginine residues. In the first mechanism (direct membrane translocation), the arginine guanidinium groups interact with phospholipids of the plasma membrane to generate neutral ion pairs that passively diffuse across the membrane[28,29] or promote the formation of transient pores that permit the CPPs to traverse the lipid bilayer.[30,31] In the second

**Received:** April 5, 2014
**Revised:** May 27, 2014
**Published:** June 4, 2014

   dx.doi.org/10.1021/bi5004102 | *Biochemistry* 2014, 53, 4034−4046

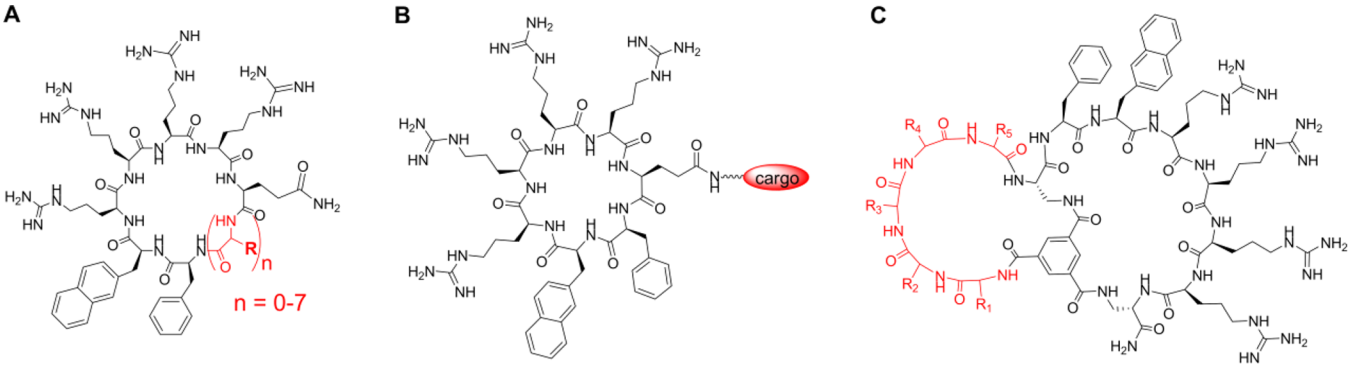


**Figure 1.** Structures showing cargo attachment during endocyclic (A), exocyclic (B), and bicyclic (C) delivery of cargos (colored red) by cFΦR$_4$.

mechanism, CPPs associate with cell surface glycoproteins and membrane phospholipids, internalize into cells through endocytosis,[32−36] and subsequently exit from endosomes into the cytoplasm. Taken together, a majority of data show that at low CPP concentrations, cellular uptake occurs mostly through endocytosis, whereas direct membrane translocation becomes prevalent at concentrations above 10 μM.[37] However, the mechanism(s) of entry and the efficiency of uptake may vary with CPP identity, cargo, cell type, and other factors.[38,39]

CPPs that enter cells via endocytosis must exit from endocytic vesicles to reach the cytosol. Unfortunately, the endosomal membrane has proven to be a significant barrier toward cytoplasmic delivery by these CPPs; often a negligible fraction of the peptides escapes into the cell interior.[40−42] For example, even in the presence of the fusogenic hemagglutinin peptide HA2, which has been demonstrated to enhance endosomal cargo release, >99% of a Tat−Cre fusion protein remains entrapped in macropinosomes 24 h after initial uptake.[35] Recently, two new types of CPPs with improved endosomal escape efficiencies have been discovered. Appelbaum et al. showed that folded miniature proteins containing a discrete pentaarginine motif were able to effectively overcome endosomal entrapment and reach the cytosol of mammalian cells.[42] This motif consists of five arginines across three turns of an α-helix, and proteins containing this motif were released from early (Rab5$^+$) endosomes into the cell interior. We and others found that cyclization of certain arginine-rich CPPs enhances their cellular uptake.[43−46] Small amphipathic cyclic peptides such as cyclo(FΦRRRRQ) (cFΦR$_4$, where Φ is L-2-naphthylalanine) are internalized by mammalian cells in an energy-dependent manner and enter the cytoplasm and nucleus with efficiencies 2−5-fold higher than that of nonaarginine (R$_9$).[43] Moreover, membrane impermeable cargos such as phosphopeptides can be inserted into the cFΦR$_4$ ring, resulting in their delivery into the cytoplasm of target cells. However, insertion of a cargo into the cyclic peptide ring, which we term the "endocyclic" delivery method (Figure 1A), is limited to relatively short peptides (no more than seven amino acids), as large rings, for yet unknown reasons, display poor internalization efficiency.[43]

To gain insight into the cFΦR$_4$ mechanism of action and potentially design cyclic CPPs of still higher efficiency, in this study we investigated the internalization mechanism of cFΦR$_4$ through the use of artificial membranes and pharmacologic agents as well as genetic mutations that perturb various endocytic events. Our data show that cFΦR$_4$ binds directly to the plasma membrane phospholipids and enters cells through endocytosis. Like the miniature proteins displaying the pentaarginine motif,[42] cFΦR$_4$ escapes from the early endosomes into the cytosol. We also examined the ability of cFΦR$_4$ to deliver a wide range of cargo molecules, including linear peptides of varying charges, cyclic peptides, and large proteins, into the cytoplasm of mammalian cells by exocyclic [attachment of cargo to the Gln side chain (Figure 1B)] or bicyclic [fusion of the cFΦR$_4$ and cyclic cargo rings (Figure 1C)] delivery methods. We found that cFΦR$_4$ is remarkably tolerant to the size and nature of cargos and efficiently transported all of the cargos tested into the cytoplasm and nucleus of mammalian cells. In addition, cFΦR$_4$ exhibits superior stability against proteolysis over linear CPPs but minimal cytotoxicity. cFΦR$_4$ therefore provides a practically useful transporter for cytosolic cargo delivery as well as a system for investigating the mechanism of early endosomal cargo release.

## MATERIALS AND METHODS

**Materials.** Reagents for peptide synthesis were purchased from Advanced ChemTech (Louisville, KY), NovaBiochem (La Jolla, CA), or Anaspec (San Jose, CA). 2,2′-Dipyridyl disulfide, Lissamine rhodamine B sulfonyl chloride, fluorescein isothiocyanate (FITC), dexamethasone (Dex), coenzyme A trilithium salt, FITC-labeled dextran (dextran$^{FITC}$), and human serum were purchased from Sigma-Aldrich (St. Louis, MO). Cell culture media, fetal bovine serum (FBS), penicillin/streptomycin, 0.25% trypsin-ethylenediaminetetraacetic acid, Hoescht 33342, Alexa488-labeled dextran (dextran$^{Alexa488}$), Dulbecco's phosphate-buffered saline (DPBS) (2.67 mM potassium chloride, 1.47 mM potassium phosphate monobasic, 137 mM sodium chloride, and 8.06 mM sodium phosphate dibasic), and Lipofectamine 2000 were purchased from Invitrogen (Carlsbad, CA). PD-10 desalting columns were purchased from GE-Healthcare (Piscataway, NJ). Nuclear staining dye DRAQ5 was purchased from Thermo Scientific (Rockford, IL), while the cell proliferation kit [3-(4,5-dimethylthiazol-2-yl)-2,5-diphenyltetrazolium bromide (MTT)] was purchased from Roche (Indianapolis, IN). The anti-phosphotyrosine (pY) antibody (clone 4G10) was purchased from Millipore (Temecula, CA).

**Peptide Synthesis and Labeling.** The details of peptide synthesis are described in the Supporting Information. Peptide labeling with FITC was performed by dissolving the purified peptide (~1 mg) in 300 μL of 1:1:1 (v/v) dimethyl sulfoxide (DMSO)/dimethylformamide (DMF)/150 mM sodium bicarbonate (pH 8.5) mixture and mixing that solution with 10 μL of FITC in DMSO (100 mg/mL). After 20 min at room temperature, the reaction mixture was subjected to reversed-phase high-performance liquid chromatography (HPLC) on a


dx.doi.org/10.1021/bi5004102 | Biochemistry 2014, 53, 4034−4046

$C_{18}$ column to isolate the FITC-labeled peptide. To generate rhodamine- and Dex-labeled peptides (Figure S1 of the Supporting Information), an $N^{\varepsilon}$-4-methoxytrityl-L-lysine was added to the C-terminus. After solid-phase peptide synthesis, the lysine side chain was selectively deprotected using 1% (v/v) trifluoroacetic acid in $CH_2Cl_2$. The resin was incubated with Lissamine rhodamine B sulfonyl chloride and DIPEA (5 equiv each) in DMF overnight. The peptides were fully deprotected as described in the Supporting Information, triturated with diethyl ether, and purified by HPLC. The Dex-labeled peptide was produced by incubating the resin with a mixture of dexamethasone-21-thiopropionic acid, HBTU, and DIPEA (5, 5, and 10 equiv, respectively) in DMF for 3 h.[42] The peptide was then deprotected, triturated, and purified by HPLC. Bicyclic peptides, phosphocoumaryl aminopropionic acid (pCAP), and pCAP-containing peptides (PCPs) were synthesized as previously described.[47−49] The authenticity of each peptide was confirmed by matrix-assisted laser desorption ionization time-of-flight mass spectrometry.

**Preparation of cFΦR$_4$−Protein Conjugates.** Peptide cFΦR$_4$ containing a C-terminal cysteine [cFΦR$_4$-SH, ∼10 μmol (Figure S2 of the Supporting Information)] was dissolved in 1 mL of degassed DPBS and mixed with 2,2′-dipyridyl disulfide (5 equiv) dissolved in acetone (0.5 mL). After 2 h at room temperature, the reaction product cFΦR$_4$-SS-Py was purified by reversed-phase HPLC. The product was incubated with coenzyme A (2 equiv) in DPBS for 2 h. The resulting cFΦR$_4$-SS-CoA adduct was purified again by reversed-phase HPLC. Green fluorescent protein (GFP) containing an N-terminal ybbR tag (VLDSLEFIASKL) and a C-terminal six-histidine tag was expressed in *Escherichia coli* and purified as previously described.[50] Next, ybbR-GFP (30 μM), cFΦR$_4$-SS-CoA (30 μM), and phosphopantetheinyl transferase Sfp (0.5 μM) were mixed in 50 mM HEPES (pH 7.4) and 10 mM $MgCl_2$ (total volume of 1.5 mL) and incubated at 37 °C for 15 min. The labeled protein, cFΦR$_4$-S-S-GFP (Figure S2 of the Supporting Information), was separated from unreacted cFΦR$_4$-SS-CoA by passing the reaction mixture through a PD-10 desalting column. GFP conjugated to Tat (Tat-S-S-GFP) and cFΦR$_4$-conjugated PTP1B (cFΦR$_4$-PTP1B) were prepared in a similar fashion (Figure S3 of the Supporting Information).

**Cell Culture and Transfection.** HEK293, HeLa, MCF-7, NIH 3T3, and A549 cells were maintained in medium consisting of Dulbecco's modified Eagle's medium (DMEM), 10% FBS, and 1% penicillin/streptomycin. H1650 and H1299 cells were grown in RPMI-1640 supplemented with 10% FBS and 1% penicillin/streptomycin. Cells were cultured in a humidified incubator at 37 °C with 5% $CO_2$. For the transfection of HeLa cells, cells were seeded onto a 96-well plate at a density of 10000 cells/well. Following attachment, cells were transfected with plasmids encoding the Rab5-green fluorescent protein fusion (Rab5-GFP, a gift from P. Di Camilli), Rab7-GFP (Addgene plasmid 28047, Q. Zhong), the glucocorticoid receptor (C638G)-GFP fusion (GR-GFP),[51] DsRed-Rab5 WT (Addgene plasmid 13050, R. Pagano), or DsRed-Rab5$^{Q79L}$ (Addgene plasmid 29688, E. DeRobertis) following manufacturer's protocols for Lipofectamine 2000.

**Confocal Microscopy.** To examine the colocalization between rhodamine-labeled cyclic peptide (cFΦR$_4^{Rho}$) and Rab5$^+$ or Rab7$^+$ endosomes, HeLa cells transfected with Rab5-GFP or Rab7-GFP were plated (200 μL, $10^4$ cells/well, 96-well glass bottom MatriPlates) the day prior to the experiment. On the day of the experiment, HeLa cells were treated with 1 μM cFΦR$_4^{Rho}$ in DMEM supplemented with 300 nM Hoescht 33342 for 30 min. After that, the cells were washed with HKR buffer [10 mM HEPES (pH 7.4), 140 mM NaCl, 2 mM KCl, 1 mM $CaCl_2$, and 1 mM $MgCl_2$] and imaged using a PerkinElmer LiveView spinning disk confocal microscope.

For the GR translocation assay, HeLa cells transfected with GR-GFP were plated as described above.[51] The cells were treated for 30 min with DMEM containing 1 μM Dex or Dex-peptide conjugate and 300 nM Hoescht 33342 and imaged using a Zeiss Axiovert 200M epifluorescence microscope outfitted with a Ziess Axiocam mRM camera and an EXFO-Excite series 120 Hg arc lamp. The translocation ratio (the ratio of mean GFP intensity in the nuclear and surrounding regions) for individual cells was measured as described in the Supporting Information. To examine the effect of endocytosis inhibitors, transfected HeLa cells were pretreated for 30 min with clear DMEM containing the inhibitors before incubation with Dex or Dex-peptide conjugates. To test whether Rab5 activity is required for endosomal escape, HeLa cells were transfected with GR-GFP and DsRed-Rab5 WT or DsRed-Rab5$^{Q79L}$ before being treated with Dex or the Dex-peptide conjugate and imaged as described above.[42]

To examine the internalization of rhodamine-labeled peptides, $5 \times 10^4$ HEK293 cells were plated in a 35 mm glass-bottom microwell dish (MatTek). On the day of the experiment, the cells were incubated with the peptide solution (5 μM) and 0.5 mg/mL dextran$^{FITC}$ at 37 °C for 2 h. The cells were gently washed with DPBS twice and imaged on a Visitech Infinity 3 Hawk 2D-array live cell imaging confocal microscope. To detect the internalization of pCAP-containing peptides, HEK293 cells were similarly plated and incubated with the peptide solution (5 μM) at 37 °C for 60 min. After removal of the medium, the cells were gently washed with DPBS containing sodium pervanadate (1 mM) twice and incubated for 10 min in DPBS containing 5 μM nuclear staining dye DRAQ5. The resulting cells were washed with DPBS twice and imaged on a spinning disk confocal microscope (UltraView Vox CSUX1 system). To monitor GFP internalization, $5 \times 10^4$ HEK293 cells were seeded in a 35 mm glass-bottom microwell dish and cultured overnight. Cells were treated with CPP-S-S-GFP (1 μM) at 37 °C for 2 h. After removal of the medium, the cells were incubated in DPBS containing 5 μM DRAQ5 for 10 min. The cells were washed with DPBS twice and imaged on a Visitech Infinity 3 Hawk 2D-array live cell imaging confocal microscope.

**Flow Cytometry.** To quantify the delivery efficiencies of pCAP-containing peptides, HeLa cells were cultured in six-well plates ($5 \times 10^5$ cells per well) for 24 h. On the day of the experiment, the cells were incubated with 10 μM pCAP-containing peptide in clear DMEM with 1% FBS at 37 °C for 2 h. The cells were washed with DPBS containing 1 mM sodium pervanadate, detached from plate with 0.25% trypsin, suspended in DPBS containing 1% bovine serum albumin, and analyzed on a BD FACS Aria flow cytometer with excitation at 355 nm. Data were analyzed with Flowjo (Tree Star) The experimental procedure for estimating the effect of the cyclic peptide on endocytosis is described in the Supporting Information.

**Immunoblotting.** NIH 3T3 cells were cultured in full growth medium to reach 80% confluence. The cells were starved in serum free medium for 3 h and treated with different concentrations of cFΦR$_4$-PTP1B or untagged PTP1B for 2 h,

followed by a 30 min incubation in medium supplemented with 1 mM sodium pervanadate. The solutions were removed and the cells washed twice with cold DPBS. The cells were detached and lysed in 50 mM Tris-HCl (pH 7.4), 150 mM NaCl, 1% NP-40, 10 mM sodium pyrophosphate, 5 mM iodoacetic acid, 10 mM NaF, 1 mM ethylenediaminetetraacetic acid, 2 mM sodium pervanadate, 0.1 mg/mL phenylmethanesulfonyl fluoride, 1 mM benzamidine, and 0.1 mg/mL trypsin inhibitor. After being incubated on ice for 30 min, the cell lysate was centrifuged at 15000 rpm for 25 min in a microcentrifuge. The total cellular proteins were separated by sodium dodecyl sulfate−polyacrylamide gel electrophoresis (SDS−PAGE) and transferred electrophoretically to a polyvinylidene fluoride membrane, which was immunoblotted using anti-pY antibody 4G10.

## RESULTS AND DISCUSSION

**cFΦR$_4$ Enters Cells via Endocytosis.** We previously observed that cFΦR$_4$ fails to enter cells at 4 °C or in the presence of sodium azide, suggesting that energy-dependent endocytic processes mediate its cell entry.[43] However, other cyclic CPPs have been reported to enter cells by direct membrane translocation.[44,45] To further test the role of endocytosis and intracellular trafficking during the cellular uptake of cFΦR$_4$, we examined the extent of colocalization between cFΦR$_4^{Rho}$ (Table 1, compound **1**) and GFP-tagged Rab proteins that have been demonstrated to localize to vesicles of the endocytic system. Rab5 is a small Rab family GTPase that is primarily localized to early endosomal membranes, whereas Rab7 is predominantly localized to the membranes of late endosomes.[52,53] HeLa cells overexpressing GFP-Rab5 or GFP-Rab7 were incubated with 1 $\mu$M cFΦR$_4^{Rho}$ for 30 min and examined by spinning-disk confocal microscopy (Figure 2A). A large fraction of rhodamine B fluorescence overlapped with that of Rab5-GFP ($R_{GFP,rhodamine}$ = 0.703) and Rab7-GFP ($R_{GFP,rhodamine}$ = 0.591), indicating that cFΦR$_4^{Rho}$ is present in both early (Rab5$^+$) and late (Rab7$^+$) endosomes.

To further delineate the endocytic events required for the cytosolic delivery of cFΦR$_4$, we made use of a novel GR-GFP translocation assay[42,51,54] and examined the effects of various endocytic inhibitors on the cytosolic delivery of Dex-labeled peptides cFΦR$_4^{Dex}$ and Tat$^{Dex}$ (Figure S1 of the Supporting Information and Table 1, compounds **2** and **3**). In resting cells, GR (glucocorticoid receptor) is maintained in the cytoplasm through interactions with host chaperones.[55] Upon cytoplasmic delivery of Dex or Dex-peptide conjugates, association with the GR activates translocation from the cytoplasm into the nucleus.[56] Thus, the ratio of GR-GFP fluorescence intensity in the nucleus to that in the cytoplasm, or the translocation ratio (TR), provides a semiquantitation of the cytosolic Dex or Dex-peptide concentration. It should be noted that this assay is ideal for comparing the cytosolic concentrations of a Dex derivative under different conditions (e.g., in the absence and presence of an endocytosis inhibitor); for different Dex derivatives (e.g., cFΦR$_4^{Dex}$ and Tat$^{Dex}$), the TR may also be affected by their solubility, metabolic stability, and/or binding affinity for GR.[42,51] Incubation of HeLa cells expressing a GR-GFP fusion protein with 1 $\mu$M cFΦR$_4^{Dex}$ increased the TR from 1.17 ± 0.23 in untreated cells to 3.50 ± 0.66, confirming that a significant amount of cFΦR$_4^{Dex}$ reached the cytoplasm. Treatment of HeLa cells before and during cFΦR$_4^{Dex}$ incubation with the cell-permeable dynamin inhibitor Dynasore (Dyna), the cortical actin remodeling inhibitor *N*-ethyl-isopropyl-amiloride (EIPA), or the cholesterol-sequestering agent methyl-$\beta$-cyclodextrin (MBCD) decreased the cFΦR$_4^{Dex}$ TR to 2.35 ± 0.75, 1.86 ± 0.46, and 1.56 ± 0.39, respectively (Figure 2B and Figure S4 of the Supporting Information).[57−59] These results strongly support our previous hypothesis that cFΦR$_4$ enters cells predominantly through endocytosis,[43] and the inhibition pattern suggests the involvement of multiple endocytic mechanisms during the uptake of cFΦR$_4$.

**Table 1. Sequences of Peptides Used in This Work**

| peptide | abbreviation | peptide sequence[a] |
|---|---|---|
| 1 | cFΦR$_4^{Rho}$ | cyclo(FΦRRRRQ)-K(Rho)-NH$_2$ |
| 2 | cFΦR$_4^{Dex}$ | cyclo(FΦRRRRQ)-K(Dex)-NH$_2$ |
| 3 | Tat$^{Dex}$ | H-K(Dex)-GRKKRRQRRRPPQY-NH$_2$ |
| 4 | cFΦR$_4^{FITC}$ | cyclo(FΦRRRRQ)-K(FITC)-NH$_2$ |
| 5 | cFΦR$_4$-R$_5$ | cyclo(FΦRRRRQ)-RRRRR-K(Rho)-NH$_2$ |
| 6 | cFΦR$_4$-A$_5$ | cyclo(FΦRRRRQ)-AAAAA-K(Rho)-NH$_2$ |
| 7 | cFΦR$_4$-F$_4$ | cyclo(FΦRRRRQ)-FFFF-K(Rho)-NH$_2$ |
| 8 | cFΦR$_4$-PCP | cyclo(FΦRRRRQ)-miniPEG-DE(pCAP)LI-NH$_2$ |
| 9 | PCP | Ac-DE(pCAP)LI-NH$_2$ |
| 10 | R$_9$-PCP | Ac-RRRRRRRRR-miniPEG-DE(pCAP)LI-NH$_2$ |
| 11 | Tat-PCP | Ac-RKKRRQRRR-miniPEG-DE(pCAP)LI-NH$_2$ |
| 12 | Antp-PCP | Ac-RQIKIWFQNRRMKWKK-miniPEG-DE(pCAP)LI-NH$_2$ |
| 13 | bicyclo(FΦR$_4$-A$_5$)$^{Rho}$ | [Tm(AAAAA)K(RRRRΦF)J]-K(Rho)-NH$_2$ |
| 14 | bicyclo(FΦR$_4$-A$_7$)$^{Rho}$ | [Tm(AAAAAAA)K(RRRRΦF)J]-K(Rho)-NH$_2$ |
| 15 | bicyclo(FΦR$_4$-RARAR)$^{Rho}$ | [Tm(RARAR)K(RRRRΦF)J]-K(Rho)-NH$_2$ |
| 16 | bicyclo(FΦR$_4$-DADAD)$^{Rho}$ | [Tm(DADAD)K(RRRRΦF)J]-K(Rho)-NH$_2$ |
| 17 | monocyclo(FΦR$_4$-A$_5$)$^{Rho}$ | cyclo(AAAAARRRRΦF)-K(Rho)-NH$_2$ |
| 18 | monocyclo(FΦR$_4$-A$_7$)$^{Rho}$ | cyclo(AAAAAAARRRRΦF)-K(Rho)-NH$_2$ |
| 19 | cFΦR$_4$ | cyclo(FΦRRRRQ) |
| 20 | R$_9$ | H-RRRRRRRRR-OH |
| 21 | Tat | H-YGRKKRRQRRR-OH |
| 22 | Antp | H-RQIKIWFQNRRMKWKK-OH |

[a]Abbreviations: Φ, L-2,3-naphthylalanine; J, L-2,3-diaminopropionic acid; Rho, rhodamine B; Dex, dexamethasone; FITC, fluorescein isothiocyanate; miniPEG, 8-amino-3,6-dioxaoctanoic acid; pCAP, phosphocoumaryl aminopropionic acid; Tm, trimesoyl.

**cFΦR$_4$ Escapes from Early Endosomes into the Cytoplasm.** The presence of intense, diffuse fluorescence throughout the cytoplasm and nucleus of cells treated with fluorescently labeled cFΦR$_4$ indicates that cFΦR$_4$ efficiently escapes from the endosome (ref 43 and *vide infra*). In an attempt to understand why cFΦR$_4$ possesses this unusual property among CPPs, we again made use of the GR-GFP translocation assay to examine the effect of downstream endocytic perturbations on the cytoplasmic delivery of cFΦR$_4^{Dex}$. Pretreatment of HeLa cells with the endosomal vesicular ATPase inhibitor bafilomycin (Baf)[60] prior to the addition of cFΦR$_4^{Dex}$ decreased the TR to 2.66 ± 0.62, suggesting that endosomal acidification facilitates the release of cFΦR$_4^{Dex}$ into the cytoplasm. Blocking the maturation of Rab5$^+$ vesicles by pretreating cells with the phosphatidylinositol 3-


dx.doi.org/10.1021/bi5004102 | *Biochemistry* 2014, 53, 4034−4046

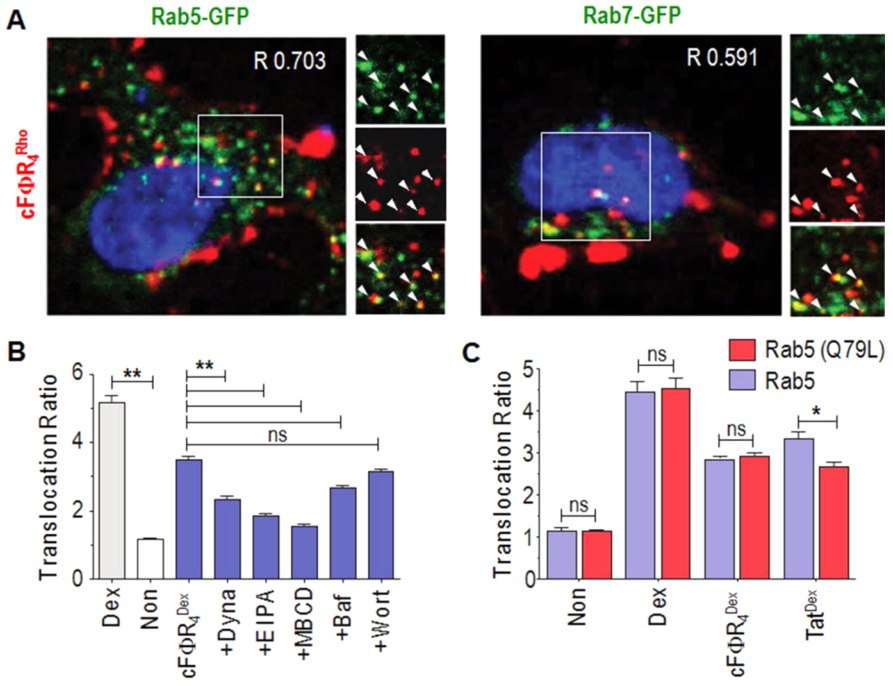


**Figure 2.** cFΦR$_4$ enters cells through endocytosis, localizes to Rab5$^+$ and Rab7$^+$ endosomes, and releases from early endosomes into cytoplasm. (A) Colocalization between Rab5-GFP (left) or Rab7-GFP (right) and cFΦR$_4^{Rho}$ (red) HeLa cells stained with Hoescht 33342 (blue). (B) Translocation of GR-GFP after treatment with 1 $\mu$M Dex or cFΦR$_4^{Dex}$ in the presence and absence of 80 $\mu$M Dynasore (Dyna), 50 $\mu$M *N*-ethyl-isopropyl-amiloride (EIPA), 5 mM methyl-$\beta$-cyclodextrin (MBCD), 200 nM wortmannin (Wort), or 200 nM bafilomycin (Baf). (C) Translocation of GR-GFP after treatment with 1 $\mu$M Dex or cFΦR$_4^{Dex}$ upon overexpression of WT Rab5 or Rab5(Q79L). *$p \leq 0.01$; **$p \leq 0.001$; ns, not significant (two-tailed *t* test).

kinase inhibitor wortmannin (Wort)[61] had an only minor effect on the TR (from 3.50 ± 0.66 to 3.15 ± 0.55), supporting the idea that cFΦR$_4^{Dex}$ is released from early Rab5$^+$ endosomes. To further test whether endosomal maturation is required for cytosolic delivery, we overexpressed GTPase-inactive Rab5 mutant, Rab5(Q79L), which halts endosomal maturation at the Rab5$^+$ stage.[62] Rab5(Q79L) overexpression significantly reduced the TR for Tat$^{Dex}$, which has previously been shown to be released from late endosomes[42] but had no effect on either free Dex or cFΦR$_4^{Dex}$ (Figure 2C and Figure S5 of the Supporting Information), confirming that cFΦR$_4$ is released from early endosomes into the cytoplasm. Interestingly, miniature proteins containing a pentaarginine motif on an $\alpha$-helix, another system shown to efficiently escape from the endosome, are also released from the early endosome.[42] R$_9$ was previously shown to exit the endocytic pathway after the miniature proteins but prior to Tat.[42] It appears that compared to other cationic CPPs, cFΦR$_4$ is less dependent on endosomal acidification for release and thus able to exit from the less acidic early endosomes.

**cFΦR$_4$ Binds to Membrane Phospholipids.** It was previously observed that incubation of 1 $\mu$M FITC-labeled cyclic peptide cFΦR$_4^{FITC}$ (Table 1, compound **4**) with vesicles containing negatively charged phospholipids [90% phosphatidylcholine (PC) and 10% phosphatidylglycerol (PG)] resulted in quenching of the peptide fluorescence, consistent with direct binding of cFΦR$_4$ to phospholipids.[43] To test the potential role of membrane binding during endocytic uptake of CPPs, we prepared SUVs that mimic the outer membrane of mammalian cells (45% PC, 20% phosphatidylethanolamine, 20% sphingomyelin, and 15% cholesterol) and tested them for binding to FITC-labeled cFΦR$_4$, R$_9$, and Tat (each at 100 nM) by a fluorescence polarization (FP) assay. cFΦR$_4$ bound to the neutral SUVs with an EC$_{50}$ value (lipid concentration at which half of cFΦR$_4^{FITC}$ is bound) of 2.1 ± 0.1 mM (Figure 3A). R$_9$ showed much weaker binding to the artificial membrane (EC$_{50}$ > 10 mM), whereas Tat did not bind at all. We next tested the CPPs for binding to heparan sulfate, which was previously

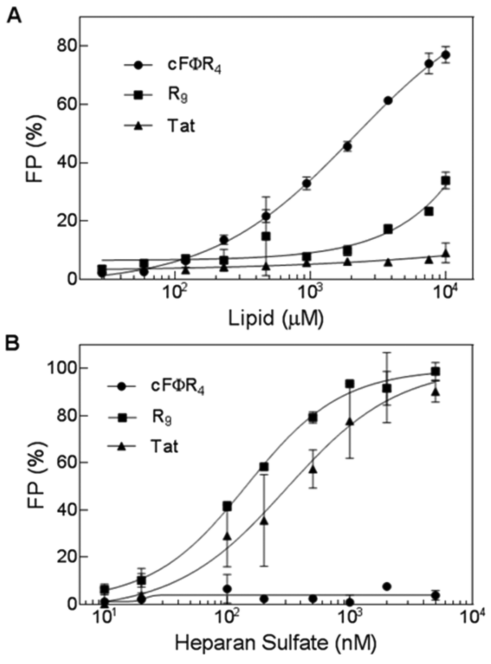


**Figure 3.** Binding of FITC-labeled cFΦR$_4$, R$_9$, and Tat to SUV (A) and heparan sulfate (B).


dx.doi.org/10.1021/bi5004102 | *Biochemistry* 2014, 53, 4034−4046

proposed to be the primary binding target of cationic CPPs.[36,63−67] As expected, $R_9$ and Tat both bound to heparan sulfate with high affinity, having $EC_{50}$ values of 144 and 304 nM, respectively (Figure 3B). Under the same condition, cFΦ$R_4$ showed no detectable binding to heparan sulfate. Our results are in agreement with the previous observations that nonamphipathic cationic CPPs (e.g., Tat and $R_9$) bind tightly with cell surface proteoglycans (e.g., heparan sulfate) but only weakly with membrane lipids.[67] The insufficient number of positive charges of cFΦ$R_4$ is likely responsible for its lack of strong electrostatic interaction with heparan sulfate. On the other hand, the amphipathic nature and the more rigid cyclic structure of cFΦ$R_4$ should facilitate its binding to neutral lipid membranes. These data, together with the inhibition pattern by various endocytic inhibitors described above, suggest that cFΦ$R_4$ binds directly to the plasma membrane phospholipids and is internalized by all of the endocytic mechanisms in a piggyback manner.

**Intracellular Delivery of Peptidyl Cargos.** Because endocyclic delivery by cFΦ$R_4$ is limited to a heptapeptide or smaller cargos,[43] in this study we tested the ability of cFΦ$R_4$ to deliver cargos of varying sizes and physicochemical properties attached to the Gln side chain (Figure 1B, exocyclic delivery). We first covalently attached positively charged (RRRRR), neutral (AAAAA), hydrophobic (FFFF), and negatively charged [DE(pCAP)LI] peptides to cFΦ$R_4$ (Table 1, compounds **5**−**8**, respectively). The first three peptides were labeled with rhodamine B at a C-terminal lysine side chain (Figure S1 of the Supporting Information), and their internalization into HEK293 cells was examined by live cell confocal microscopy. Cells incubated for 2 h with 5 μM peptide cFΦ$R_4$-$A_5$ (Figure 4A) or cFΦ$R_4$-$R_5$ (Figure 4B) showed

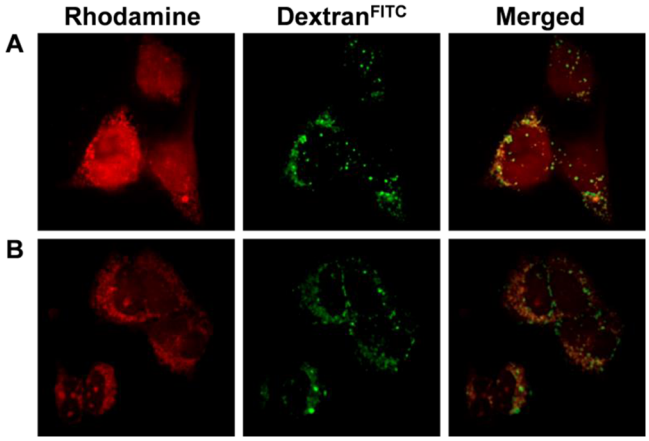


**Figure 4.** Representative live cell confocal images of HEK293 cells treated for 2 h with rhodamine B-labeled peptides and fluid-phase uptake marker dextran$^{FITC}$. (A) Cells treated with 5 μM cFΦ$R_4$-$A_5$ and dextran$^{FITC}$ in the same Z section. (B) Same as panel A but with 5 μM cFΦ$R_4$-$R_5$.

evidence of both punctate and diffuse fluorescence, with the latter distributed almost uniformly throughout the cell. In contrast, the fluid-phase endocytic marker dextran$^{FITC}$ displayed predominantly punctate fluorescence, indicative of endosomal localization. The diffuse rhodamine fluorescence suggests that a fraction of the peptides reached the cytosol and nucleus of the cells. Co-incubation of cells with cFΦ$R_4$ (1 μM) and dextran$^{Alexa488}$ increased the level of internalization of the endocytic marker by 15% (Figure S6 of the Supporting Information), suggesting that cFΦ$R_4$ activates endocytosis in cultured cells. cFΦ$R_4$-$F_4$ could not be tested because of its poor aqueous solubility.

Peptide cFΦ$R_4$-DE(pCAP)LI [cFΦ$R_4$-PCP (Figure S1 of the Supporting Information)] was designed to test the ability of cFΦ$R_4$ to deliver negatively charged cargos as well as to compare the cytoplasmic delivery efficiency of cFΦ$R_4$ with those of other widely used CPPs such as $R_9$, Tat, and penetratin (Antp). Thus, untagged PCP [Ac-DE(pCap)LI-$NH_2$] and PCP conjugated to $R_9$ ($R_9$-PCP), Tat (Tat-PCP), and Antp (Antp-PCP) (Table 1, compounds **9**−**12**, respectively) were also prepared. Note that cFΦ$R_4$-PCP carries a net charge of zero at physiological pH. pCAP is nonfluorescent but, upon entering the cell interior, should be rapidly dephosphorylated by endogenous protein tyrosine phosphatases (PTPs) to produce a fluorescent product, coumaryl aminopropionic acid (CAP, excitation at 355 nm and emission at 450 nm).[48,49] When assayed against a PTP panel *in vitro*, all four CPP-PCP conjugates were efficiently dephosphorylated (Table S1 of the Supporting Information). This assay detects only the CPP cargo inside the cytoplasm and nucleus, where the catalytic domains of all known mammalian PTPs are localized.[68] Further, CAP is fluorescent only in its deprotonated state ($pK_a$ = 7.8); even if some dephosphorylation occurs inside the endosome (pH 6.5−4.5) or lysosome (pH 4.5), it would contribute little to the total fluorescence (Figure S7 of the Supporting Information). Treatment of HEK293 cells with 5 μM cFΦ$R_4$-PCP for 60 min resulted in diffuse blue fluorescence throughout the cell, suggesting that cFΦ$R_4$-PCP reached the cell interior, whereas the untagged PCP failed to enter cells under the same condition (Figure 5A). When HEK293 cells were pretreated with the PTP inhibitor sodium pervanadate for 1 h prior to incubation with cFΦ$R_4$-PCP (5 μM), the CAP fluorescence in the cells diminished to background levels. HEK293 cells treated with $R_9$-PCP, Antp-PCP, or Tat-PCP under identical conditions showed weak fluorescence, consistent with the poor ability of these peptides to access the cell interior (Figure 5A). To quantify the relative intracellular PCP delivery efficiency, HeLa cells were treated with each peptide and analyzed by fluorescence-activated cell sorting (Figure 5B). cFΦ$R_4$-PCP was most efficiently internalized by the HeLa cells, with a mean fluorescence intensity (MFI) of 3510 arbitrary units (AU), whereas $R_9$-PCP, Antp-PCP, Tat-PCP, and untagged PCP produced MFI values of 960, 400, 290, and 30 AU, respectively (Figure 5C). Again, when cells were treated with cFΦ$R_4$-PCP in the presence of sodium pervanadate, the amount of CAP fluorescence was reduced to near background levels (70 AU). Thus, cFΦ$R_4$ is capable of delivering peptidyl cargos of varying physicochemical properties into the cytoplasm with efficiencies 3.7−12-fold higher than those of $R_9$, Antp, and Tat.

**Intracellular Delivery of Cyclic Peptides.** In recent years, there has been much interest in cyclic peptides as therapeutic agents and biomedical research tools.[69,70] For example, cyclic peptides are effective for inhibition of protein−protein interactions,[47,71−73] which are challenging targets for conventional small molecules. A major obstacle in developing cyclic peptide therapeutics is that they are generally impermeable to the cell membrane.[74−76] Our attempt to deliver cyclic peptides by cFΦ$R_4$ by the endocyclic method had only limited success; an increase in cargo size from one to seven residues led to progressively poorer cellular uptake, likely because the larger, more flexible rings bind more poorly to the cell membrane.[43]


dx.doi.org/10.1021/bi5004102 | *Biochemistry* 2014, 53, 4034−4046

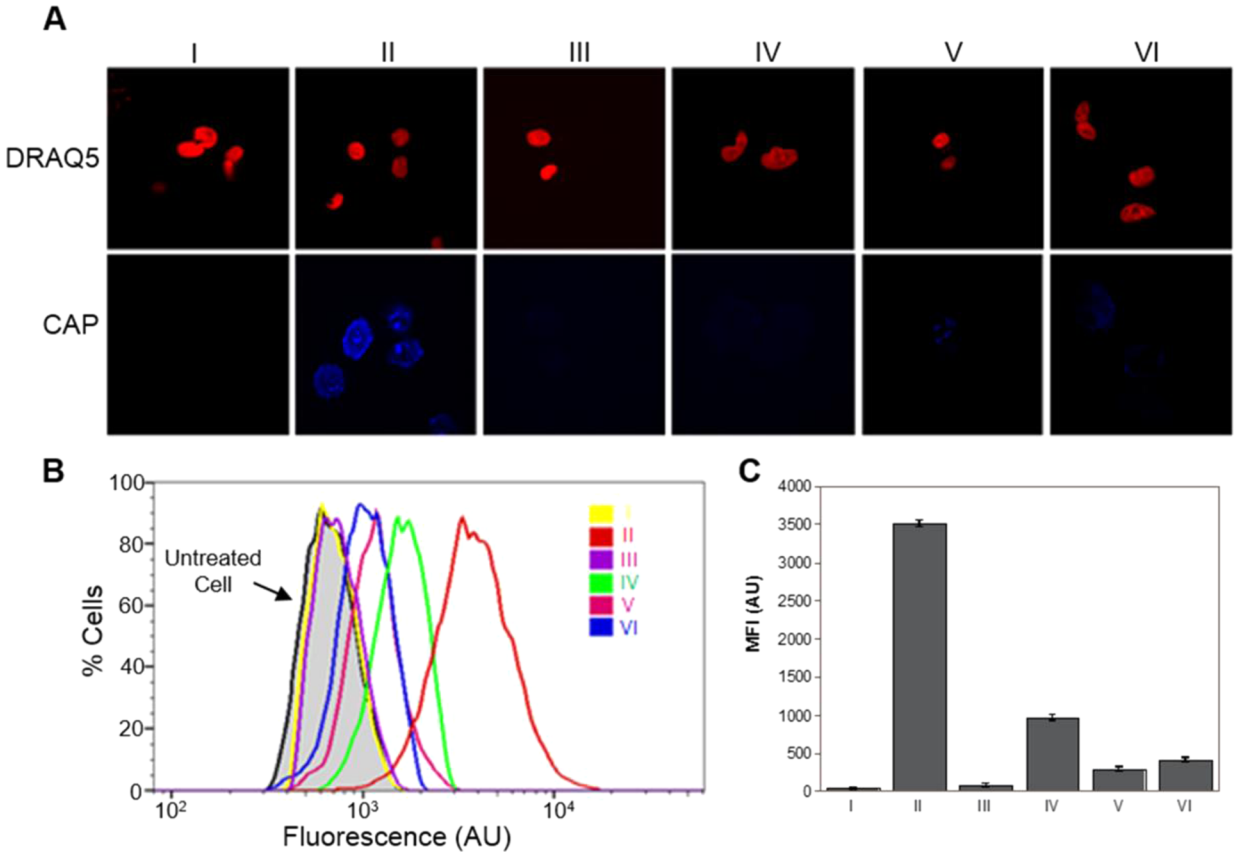


**Figure 5.** Internalization of pCAP-containing peptides into cultured cells: (I) untagged PCP, (II) cFΦ$R_4$-PCP, (III) cFΦ$R_4$-PCP and $Na_3VO_4$, (IV) $R_9$-PCP, (V) Tat-PCP, and (VI) Antp-PCP. (A) Representative live cell confocal images of HEK293 cells treated with 5 $\mu$M peptides. The top panel shows the nuclear stain with DRAQ5 and the bottom panel CAP fluorescence in the same *Z* section. (B) Flow cytometry of HeLa cells treated with 0 or 10 $\mu$M peptides. (C) CAP fluorescence from panel B after subtraction of background fluorescence (untreated cells).

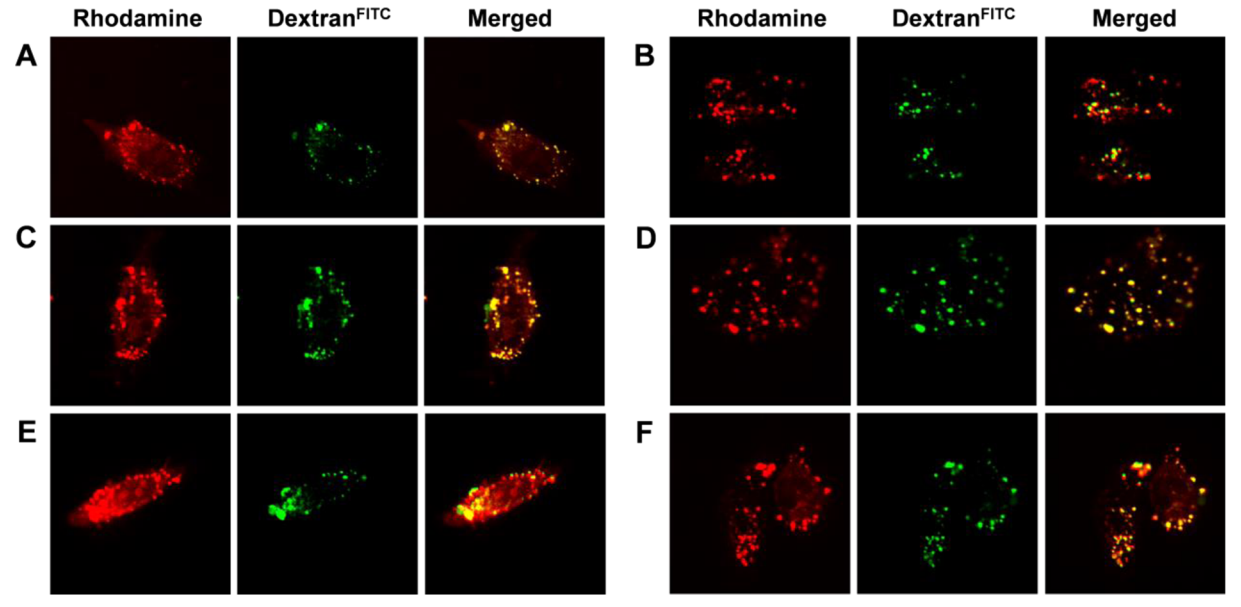


**Figure 6.** Representative live cell confocal microscopic images of HEK293 cells treated for 2 h with rhodamine B-labeled peptides (5 $\mu$M each) and fluid-phase endocytosis marker dextran$^{FITC}$ (0.5 mg/mL). The red fluorescence of rhodamine B and the green fluorescence of dextran$^{FITC}$ from the same *Z* section and their merged image are shown in each panel. The enlarged images of a typical cell(s) are shown in each case to show the intracellular distribution of the internalized peptides: (A) cells treated with bicyclo(FΦ$R_4$-$A_5$)$^{Rho}$, (B) cells treated with monocyclo(FΦ$R_4$-$A_5$)$^{Rho}$, (C) cells treated with bicyclo(FΦ$R_4$-$A_7$)$^{Rho}$, (D) cells treated with monocyclo(FΦ$R_4$-$A_7$)$^{Rho}$, (E) cells treated with bicyclo(FΦ$R_4$-RARAR)$^{Rho}$, and (F) cells treated with bicyclo(FΦ$R_4$-DADAD)$^{Rho}$.


dx.doi.org/10.1021/bi5004102 | *Biochemistry* 2014, 53, 4034−4046

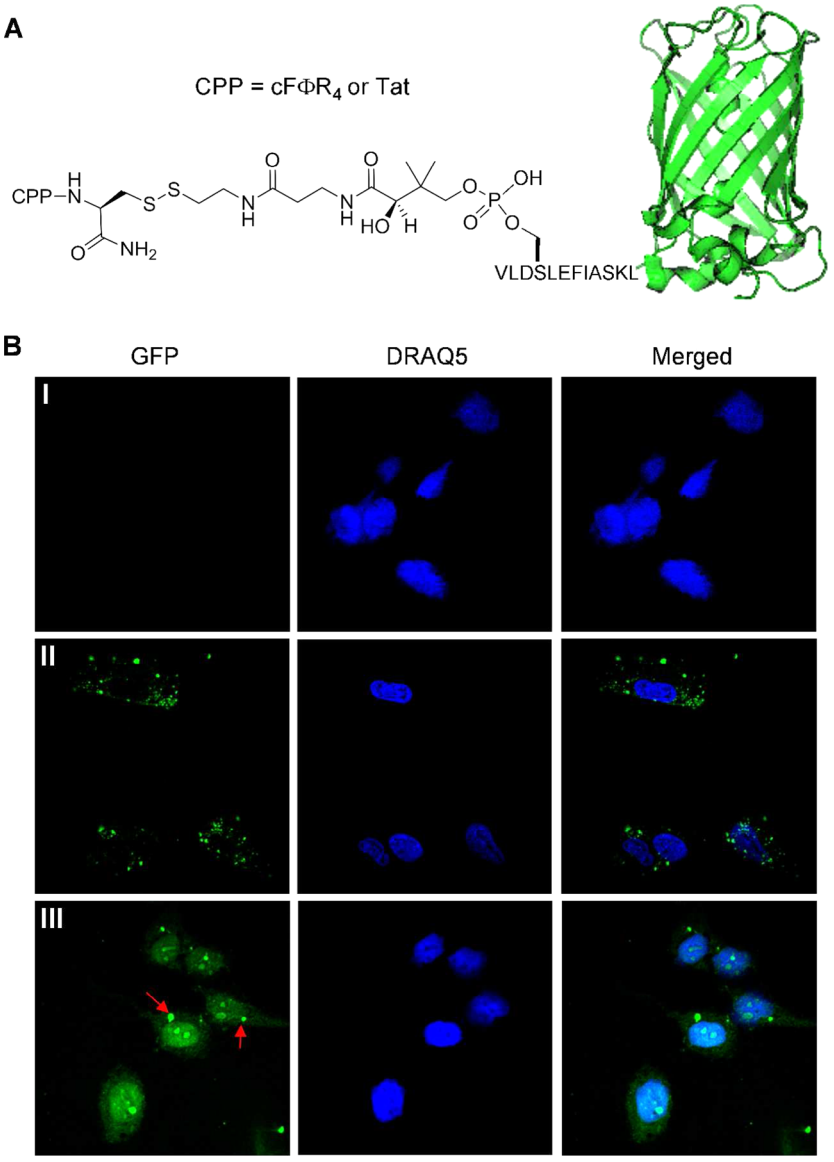


**Figure 7.** (A) Structures of CPP-S-S-GFP conjugates. (B) Live cell confocal images of HEK293 cells after treatment for 2 h with 1 $\mu$M GFP (I), Tat-S-S-GFP (II), or cF$\Phi$R$_4$-S-S-GFP (III) and nuclear stain DRAQ5. All images were recorded in the same *Z* section.

To overcome this limitation, we explored a bicyclic peptide system, in which one ring contains a CPP motif (e.g., F$\Phi$R$_4$) while the other ring consists of peptide sequences specific for the desired targets (Figure 1C). The bicyclic system should in principle be able to accommodate cargos of any size, because the cargo does not change the structure of the CPP ring and should have less impact on its delivery efficiency. The additional rigidity of a bicyclic structure should also improve its metabolic stability as well as the target binding affinity and specificity. The bicyclic peptides were readily synthesized by forming three amide bonds between a trimesoyl scaffold and three amino groups on the corresponding linear peptide [i.e., the N-terminal amine, the side chain of a C-terminal diaminopropionic acid (Dap), and the side chain of a lysine (or ornithine, Dap) imbedded between the CPP and target binding motifs].[47] To test the validity of this approach, we chose F$\Phi$R$_4$ in the C-terminal ring as the CPP moiety and peptides of different lengths and charges (AAAAA, AAAAAAA, RARAR, and DADAD) as cargo (Table 1, compounds **13**–**16**, respectively). For comparison, we also prepared two monocyclic peptides containing F$\Phi$R$_4$ as a transporter and peptides A$_5$ and A$_7$ as cargos (Table 1, compounds **17** and **18**, respectively). All of the peptides were labeled at a C-terminal lysine side chain with rhodamine B (Figure S1 of the Supporting Information), and their internalization into HEK293 cells was examined by live cell confocal microscopy. Treatment of cells with 5 $\mu$M peptide for 2 h resulted in efficient internalization of all six peptides (Figure 6), although FACS analysis indicated that the uptake of bicyclo(F$\Phi$R$_4$-A$_5$)$^{Rho}$ was ~3-fold more efficient than that of the corresponding monocyclic peptide (compound **17**). The intracellular distribution of the internalized peptides was quite different between the bicyclic and monocyclic peptides. While the four bicyclic peptides showed evidence of their presence both in the cytoplasm and nucleus (as indicated by the diffuse rhodamine fluorescence) and in the endosomes (as indicated by the fluorescence puncta), the monocyclic peptides exhibited predominantly punctate fluorescence that overlapped with that of the endocytic marker dextran$^{FITC}$. In all cases, the endocytic marker displayed only punctate fluorescence, indicating that the


dx.doi.org/10.1021/bi5004102 | *Biochemistry* 2014, 53, 4034–4046

endosomes were intact in the cells treated with the peptides. These results indicate that the increased structural rigidity of the bicyclic peptides facilitates both the initial uptake by endocytosis and endosomal release, presumably because of their improved binding to the plasma and endosomal membranes. The bicyclic system may provide a general strategy for intracellular delivery of cyclic and bicyclic peptides.

**Intracellular Delivery of Protein Cargos.** To test whether cFΦR$_4$ is capable of transporting full-length proteins into mammalian cells, we chose GFP because of its intrinsic fluorescence and attached cFΦR$_4$ to its N-terminus through a disulfide bond (Figure 7A and Figure S2 of the Supporting Information). The disulfide exchange reaction is highly specific, efficient, and reversible; upon entering the cytoplasm, the CPP-S-S-protein conjugate is expected to be rapidly reduced to release the native protein. Although cFΦR$_4$ can be directly attached to a native or engineered surface cysteine residue(s) on a cargo protein, we employed a GFP variant containing a 12-amino acid ybbR tag at its N-terminus (which was already available in our laboratory) and used phosphopantetheinyl transferase Sfp to enzymatically attach cFΦR$_4$ to the ybbR tag.[50] This permitted the attachment of a single cFΦR$_4$ unit to GFP in a site-specific manner. For comparison, we also generated a Tat-S-S-GFP conjugate in the same manner. Incubation of HEK293 cells in the presence of 1 $\mu$M cFΦR$_4$-S-S-GFP resulted in time-dependent accumulation of green fluorescence inside the cells (Figure 7B). The fluorescence signal was diffuse and present throughout the entire cell volume, but with higher concentrations in the nucleus. Some of the cells contained small spots of intense green fluorescence (indicated by arrows in Figure 7B), which may represent endosomally sequestered cFΦR$_4$-S-S-GFP or aggregated GFP inside the cell. As expected, untagged GFP was unable to enter cells, whereas Tat-S-S-GFP entered cells less efficiently than cFΦR$_4$-S-S-GFP (Figure 7B); FACS analysis of HeLa cells treated with 1 $\mu$M protein revealed a 5.5-fold higher total intracellular fluorescence for the latter. Moreover, cells treated with Tat-S-S-GFP showed predominantly punctate fluorescence in the cell periphery with no detectable fluorescence in the nuclear region, suggesting that Tat-S-S-GFP is mostly entrapped in the endosomes, in agreement with previous reports.[35] Thus, with a protein as cargo, cFΦR$_4$ also has an efficiency substantially higher than that of Tat with regard to both initial uptake and endosomal escape. Attempts to test R$_9$-S-S-GFP with cells failed because of precipitation of the conjugate.

To demonstrate the generality of cFΦR$_4$ for protein delivery, we chose next to deliver a functional enzyme, the catalytic domain of PTP1B (amino acids 1−321), into the cell interior. To show that a noncleavable linkage is also compatible with our delivery method, we conjugated cFΦR$_4$ to ybbR-tagged PTP1B via a thioether bond (cFΦR$_4$-PTP1B) (Figure S3 of the Supporting Information). An *in vitro* assay using *p*-nitrophenyl phosphate as a substrate showed that addition of the cFΦR$_4$ tag does not affect the catalytic activity of PTP1B (Table S2 of the Supporting Information). NIH 3T3 cells were incubated for 2 h in the presence of untagged PTP1B or cFΦR$_4$-PTP1B, and their global pY protein levels were analyzed by anti-pY Western blotting (Figure 8A). Treatment of the cells with cFΦR$_4$-PTP1B, but not untagged PTP1B, resulted in a concentration-dependent decrease in pY levels of most, but not all, proteins. The total cellular protein levels, as detected by Coomassie blue staining, were unchanged (Figure 8B), indicating that the

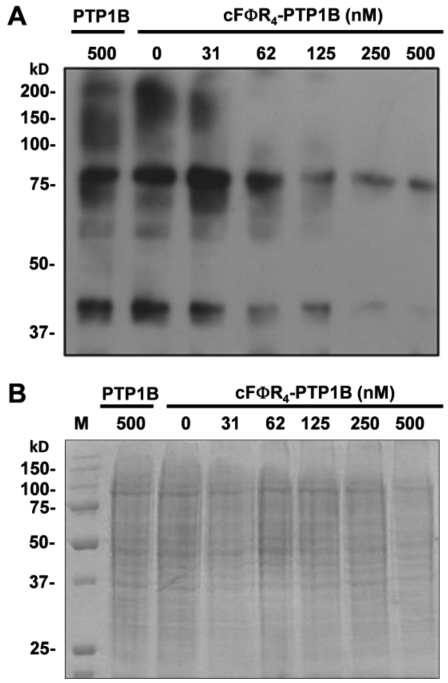


**Figure 8.** (A) Western blot analysis of the global pY protein levels of NIH 3T3 cells after treatment with 0−500 nM PTP1B or cFΦR$_4$-PTP1B (IB, anti-pY antibody 4G10). (B) The same samples as in panel A were analyzed by SDS−PAGE and Coomassie blue staining. M denotes molecular weight markers.

observed decrease in pY levels was due to dephosphorylation of the pY proteins by cFΦR$_4$-PTP1B and/or secondary effects caused by the introduction of cFΦR$_4$-PTP1B (e.g., inactivation of cellular protein tyrosine kinases). Interestingly, different proteins exhibited varying dephosphorylation kinetics. Several proteins in the 150−200 kDa range were completely dephosphorylated upon the addition of 62 nM cFΦR$_4$-PTP1B, whereas proteins of ∼80 kDa remained phosphorylated at 500 nM cFΦR$_4$-PTP1B. The changes in the pY pattern are consistent with the broad substrate specificity of PTP1B[77] and very similar to that caused by overexpression of PTP1B inside the cytosol of mammalian cells.[78] Our results indicate that cFΦR$_4$ is indeed able to deliver PTP1B into the interior of NIH 3T3 cells in the catalytically active form and to sufficient levels to dramatically perturb the cell signaling process. cFΦR$_4$ thus provides a powerful tool for introducing other functional proteins, especially proteins that cannot be genetically expressed (e.g., toxic and chemically modified proteins), into mammalian cells for studying their cellular functions.

**Stability and Cytotoxicity of cFΦR$_4$.** The relative stability of cFΦR$_4$, R$_9$, Tat, and Antp (Table 1, compounds **19**−**22**, respectively) against proteolytic degradation was determined by incubating the CPPs in 25% human serum at 37 °C and following the disappearance of the full-length peptides by reversed-phase HPLC. The cationic tryptophan-containing peptide, Antp, was least stable among the four CPPs; it was degraded at a half-life of <20 min and was completely digested after 2 h (Figure 9A). R$_9$ and Tat were slightly more stable than Antp, having half-lives of ∼30 min. In contrast, cFΦR$_4$ was remarkably stable against serum proteases. There was <10% degradation after incubation for 6 h; after incubation for 24 h in the serum, >70% of cFΦR$_4$ remained intact. Numerous other studies have also demonstrated that cyclization of peptides


dx.doi.org/10.1021/bi5004102 | *Biochemistry* 2014, 53, 4034−4046

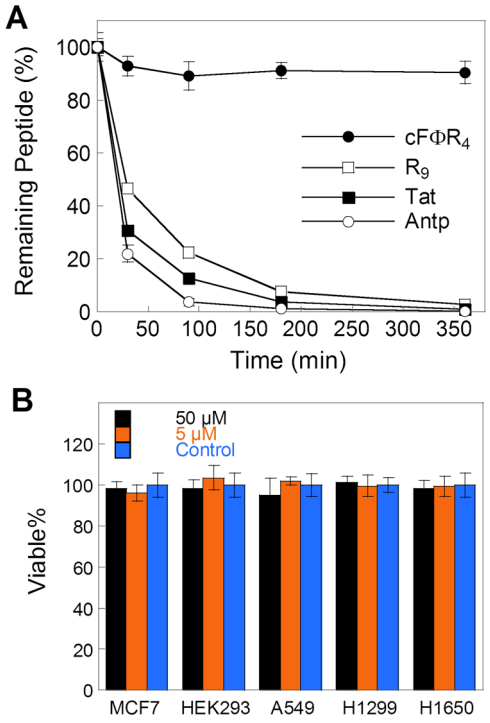


**Figure 9.** (A) Comparison of the serum stability of cFΦR$_4$, Tat, R$_9$, and Antp. (B) Cytotoxicity of cFΦR$_4$. The indicated cell lines were treated with DMSO (control) or 5 or 50 $\mu$M cFΦR$_4$ for 24 h, and the percentage of live cells was determined by the MTT assay.

greatly increases their proteolytic stabilities.[79] The potential cytotoxicity of cFΦR$_4$ was assessed by MTT assays with five different human cell lines (HEK293, MCF-7, A549, H1650, and H1299). After incubation for 24 or 48 h with up to 50 $\mu$M cFΦR$_4$, there was no significant growth inhibition for any of the cell lines (Figure 9B and Figure S8 of the Supporting Information). After 72 h, a slight growth inhibition (up to 20%) was observed at 50 $\mu$M (Figure S8 of the Supporting Information). Thus, cFΦR$_4$ is relatively nontoxic to mammalian cells.

## CONCLUSION

In this study, we demonstrate that cFΦR$_4$ is effective for the exocyclic delivery of small-molecule, peptide, and protein cargos into the cytoplasm and nucleus of mammalian cells. By using a pCAP-containing peptide as the cargo or reporter, we show that cFΦR$_4$ is 3.7−12-fold more efficient than R$_9$, Tat, and Antp for cytoplasmic cargo delivery, making cFΦR$_4$ one of the most active CPPs known to date. Although modification of polybasic CPPs such as addition of hydrophobic acyl groups has previously been reported to enhance cellular uptake by a similar magnitude,[27] to the best of our knowledge, these previous studies have not established whether the enhanced uptake translates into a similar increase in the cytoplasmic CPP concentration (our attempt to directly compare cFΦR$_4$ and the acylated CPPs was not successful, because the latter caused extensive cell death during our experiments). The pCAP-based reporter system described in this work should provide a simple, robust method for quantitatively assessing the cytoplasmic delivery efficiency of other CPPs. Several lines of evidence indicate that cFΦR$_4$ enters cells through multiple endocytic mechanisms, including its failure to enter cells at 4 °C or in the presence of sodium azide, partial overlap between the fluorescence puncta of cFΦR$_4^{Rho}$ and the fluid-phase endocytic marker dextran$^{FITC}$, colocalization of cFΦR$_4^{Rho}$ and endosomal proteins Rab5 and Rab7, and a decreased level of cFΦR$_4^{Dex}$ uptake upon administration of endocytic inhibitors. The minimal effect of the PI3K inhibitor wortmannin and the Rab5 Q79L mutation on the cytoplasmic delivery of cFΦR$_4$, in addition to the strong colocalization observed between cFΦR$_4$ and Rab5$^+$ endosomes, suggest that cFΦR$_4$ escapes from early endosomes (Figure 10). In comparison, Tat has been

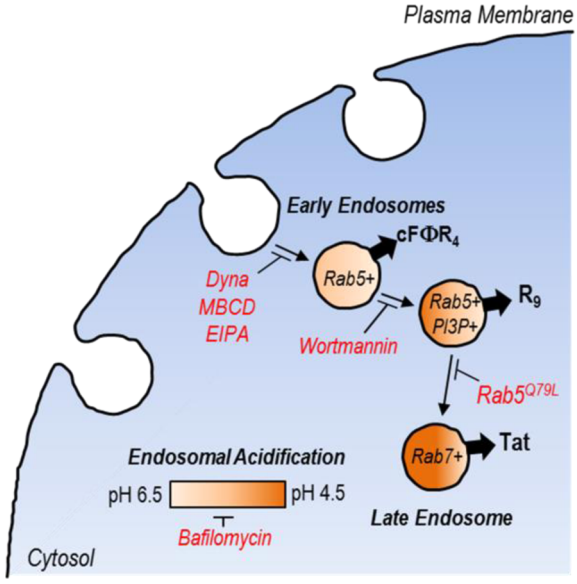


**Figure 10.** Diagram showing the points along the endocytic pathway where cFΦR$_4$, R$_9$, and Tat escape into the cytoplasm and where specific inhibitors are proposed to function.

demonstrated to enter cells through endocytosis and be released from late endosomes, while R$_9$ escapes endosomes prior to Rab7 recruitment.[42] Early endosomal release offers significant advantages, especially for peptide and protein cargos, because it minimizes cargo degradation by late endosomal and lysosomal proteases and denaturation caused by acidification during endosomal maturation. Indeed, both GFP and PTP1B delivered into the cytoplasm by cFΦR$_4$ were in their folded, active forms, as evidenced by the green fluorescence and the ability to dephosphorylate intracellular pY proteins, respectively. Additionally, because of its more rigid structure, cFΦR$_4$ is significantly more stable against proteolytic degradation than linear peptides, and because of its smaller size, cFΦR$_4$ is less expensive to synthesize and potentially less likely to interfere with the cargo function. These properties make cFΦR$_4$ a useful transporter for cytosolic delivery of small molecules to protein cargos. Direct protein delivery provides a useful research tool, e.g., for studying the cellular function of a protein, as it offers improved temporal control over DNA transfection and subsequent gene expression and allows delivery of chemically modified proteins and proteins whose overexpression causes toxicity. The ability of cFΦR$_4$ to escape from early endosomes and its simple structure may also provide an excellent system for elucidating the mechanism of endosomal escape and the factors that influence the escape efficiency.


dx.doi.org/10.1021/bi5004102 | Biochemistry 2014, 53, 4034−4046

## ■ ASSOCIATED CONTENT

### Supporting Information

Additional materials and methods for peptide synthesis, SUV preparation, FP assay, preparation of cFΦR$_4$-PTP1B, image analysis, flow cytometry analysis, the serum stability assay, and the cytotoxicity assay. This material is available free of charge via the Internet at http://pubs.acs.org.

## ■ AUTHOR INFORMATION


### Corresponding Author

*Department of Chemistry and Biochemistry, The Ohio State University, 100 W. 18th Ave., Columbus, OH 43210. E-mail: pei.3@osu.edu. Telephone: (614) 688-4068. Fax: (614) 292-1685.



### Funding

This work was supported by National Institutes of Health (NIH) Grants GM062820, GM74756, CA170741, and DE019667. J.R.L. gratefully acknowledges support from an NIH Chemistry-Biology Interface Training Program (T32GM067543).


### Notes

The authors declare no competing financial interest.

## ■ ACKNOWLEDGMENTS


We thank F. Rivera-Molina, Y. Zhu, Dr. J.-Q. Wu, and Dr. S. Cole for their assistance with confocal microscopy, Dr. D. Bong and Z. Zhou for their assistance with dynamic light scattering analysis, and Dr. A. Schepartz for helpful discussions.


## ■ REFERENCES


(1) Frankel, A. D., and Pabo, C. O. (1988) Cellular uptake of the tat protein from human immunodeficiency virus. *Cell 55*, 1189−1193.

(2) Green, M., and Loewenstein, P. M. (1988) Autonomous functional domains of chemically synthesized human immunodeficiency virus tat trans-activator protein. *Cell 55*, 1179−1188.

(3) Langel, Ü. (2011) *Cell-penetrating peptides: Methods and protocols*, p xv, Humana Press, New York.

(4) Schmidt, N., Mishra, A., Lai, G. H., and Wong, G. C. (2010) Arginine-rich cell-penetrating peptides. *FEBS Lett. 584*, 1806−1813.

(5) Futaki, S. (2005) Membrane-permeable arginine-rich peptides and the translocation mechanisms. *Adv. Drug Delivery Rev. 57*, 547−558.

(6) Stewart, K. M., Horton, K. L., and Kelley, S. O. (2008) Cell-penetrating peptides as delivery vehicles for biology and medicine. *Org. Biomol. Chem. 6*, 2242−2255.

(7) Deshayes, S., Morris, M. C., Divita, G., and Heitz, F. (2005) Cell-penetrating peptides: Tools for intracellular delivery of therapeutics. *Cell. Mol. Life Sci. 62*, 1839−1849.

(8) Goun, E. A., Pillow, T. H., Jones, L. R., Rothbard, J. B., and Wender, P. A. (2005) Molecular Transporters: Synthesis of oligoguanidinium transporters and their application to drug delivery and real-time imaging. *ChemBioChem 7*, 1497−1515.

(9) Rothbard, J. B., Garlington, S., Lin, Q., Kirschberg, T., Kreider, E., McGrane, P. L., Wender, P. A., and Khavari, P. A. (2000) Conjugation of arginine oligomers to cyclosporin A facilitates topical delivery and inhibition of inflammation. *Nat. Med. 6*, 1253−1257.

(10) Nori, A., Jensen, K. D., Tijerina, M., Kopeckova, P., and Kopecek, J. (2003) Tat-conjugated synthetic macromolecules facilitate cytoplasmic drug delivery to human ovarian carcinoma cells. *Bioconjugate Chem. 14*, 44−50.

(11) Hoyer, J., and Neundorf, I. (2012) Peptide vectors for the nonviral delivery of nucleic acids. *Acc. Chem. Res. 45*, 1048−1056.

(12) Eguchi, A., Akuta, T., Okuyama, H., Senda, T., Yokoi, H., Inokuchi, H., Fujita, S., Hayakawa, T., Takeda, K., Hasegawa, M., and Nakanishi, M. (2001) Protein transduction domain of HIV-1 Tat protein promotes efficient delivery of DNA into mammalian cells. *J. Biol. Chem. 276*, 26204−26210.

(13) Nakase, I., Akita, H., Kogure, K., Graslund, A., Langel, U., Harashima, H., and Futaki, S. (2012) Efficient Intracellular Delivery of Nucleic Acid Pharmaceuticals Using Cell-Penetrating Peptides. *Acc. Chem. Res. 45*, 1132−1139.

(14) Andaloussi, S. E., Lehto, T., Mager, I., Rosenthal-Aizman, K., Oprea, I. I., Simonson, O. E., Sork, H., Ezzat, K., Copolovici, D. M., Kurrikoff, K., Viola, J. R., Zaghloul, E. M., Sillard, R., Johansson, H. J., Said Hassane, F., Guterstam, P., Suhorutsenko, J., Moreno, P. M., Oskolkov, N., Halldin, J., Tedebark, U., Metspalu, A., Lebleu, B., Lehtio, J., Smith, C. I., and Langel, U. (2011) Design of a peptide-based vector, PepFect6, for efficient delivery of siRNA in cell culture and systemically in vivo. *Nucleic Acids Res. 39*, 3972−3987.

(15) Jeong, J. H., Mok, H., Oh, Y. K., and Park, T. G. (2009) siRNA conjugate delivery systems. *Bioconjugate Chem. 20*, 5−14.

(16) Muratovska, A., and Eccles, M. R. (2004) Conjugate for efficient delivery of short interfering RNA (siRNA) into mammalian cells. *FEBS Lett. 558*, 63−68.

(17) Wadia, J. S., and Dowdy, S. F. (2005) Transmembrane delivery of protein and peptide drugs by TAT-mediated transduction in the treatment of cancer. *Adv. Drug Delivery Rev. 57*, 579−596.

(18) Pooga, M., Kut, C., Kihlmark, M., Hallbrink, M., Fernaeus, S., Raid, R., Land, T., Hallberg, E., Bartfai, T., and Langel, U. (2001) Cellular translocation of proteins by transportan. *FASEB J. 15*, 1451−1453.

(19) Schwarze, S. R., Ho, A., Vocero-Akbani, A., and Dowdy, S. F. (1999) In vivo protein transduction: Delivery of a biologically active protein into the mouse. *Science 285*, 1569−1572.

(20) Josephson, L., Tung, C. H., Moore, A., and Weissleder, R. (1999) High-efficiency intracellular magnetic labeling with novel superparamagnetic-Tat peptide conjugates. *Bioconjugate Chem. 10*, 186−191.

(21) Gupta, B., Levchenko, T. S., and Torchilin, V. P. (2005) Intracellular delivery of large molecules and small particles by cell-penetrating proteins and peptides. *Adv. Drug Delivery Rev. 57*, 637−651.

(22) Liu, J., Zhang, Q., Remsen, E. E., and Wooley, K. L. (2001) Nanostructured materials designed for cell binding and transduction. *Biomacromolecules 2*, 362−368.

(23) Saar, K., Lindgren, M., Hansen, M., Eiriksdottir, E., Jiang, Y., Rosenthal-Aizman, K., Sassian, M., and Langel, U. (2005) Cell-penetrating peptides: A comparative membrane toxicity study. *Anal. Biochem. 345*, 55−65.

(24) Suhorutsenko, J., Oskolkov, N., Arukuusk, P., Kurrikoff, K., Eriste, E., Copolovici, D. M., and Langel, U. (2011) Cell-penetrating peptides, PepFects, show no evidence of toxicity and immunogenicity in vitro and in vivo. *Bioconjugate Chem. 22*, 2255−2262.

(25) Rueping, M., Mahajan, Y., Sauer, M., and Seebach, D. (2002) Cellular uptake studies with β-peptides. *ChemBioChem 3*, 257−259.

(26) Cooley, C. B., Trantow, B. M., Nederberg, F., Kiesewetter, M. K., Hedrick, J. L., Waymouth, R. M., and Wender, P. A. (2009) Oligocarbonate molecular transporters: Oligomerization-based syntheses and cell-penetrating studies. *J. Am. Chem. Soc. 131*, 16401−16403.

(27) Pham, W., Kircher, M. F., Weissleder, R., and Tung, C. H. (2004) Enhancing membrane permeability by fatty acylation of oligoarginine peptides. *ChemBioChem 5*, 1148−1151.

(28) Herce, H. D., and Garcia, A. E. (2007) Molecular dynamics simulations suggest a mechanism for translocation of the HIV-1 TAT peptide across lipid membranes. *Proc. Natl. Acad. Sci. U.S.A. 104*, 20805−20810.

(29) Hirose, H., Takeuchi, T., Osakada, H., Pujals, S., Katayama, S., Nakase, I., Kobayashi, S., Haraguchi, T., and Futaki, S. (2012) Transient focal membrane deformation induced by arginine-rich peptides leads to their direct penetration into cells. *Mol. Ther. 20*, 984−993.

(30) Herce, H. D., Garcia, A. E., Litt, J., Kane, R. S., Martin, P., Enrigue, N., Rebolledo, A., and Milesi, V. (2009) Arginine-rich

peptides destabilize the plasma membrane, consistent with a pore formation translocation mechanism of cell-penetrating peptides. *Biophys. J. 97*, 1917−1925.
(31) Palm-Apergi, C., Lorents, A., Padari, K., Pooga, M., and Hallbrink, M. (2009) The membrane repair response masks membrane disturbances caused by cell-penetrating peptide uptake. *FASEB J. 23*, 214−223.
(32) Richard, J. P., Melikov, K., Brooks, H., Prevot, P., Lebleu, B., and Chernomordik, L. V. (2005) Cellular uptake of unconjugated TAT peptide involves clathrin-dependent endocytosis and heparan sulfate receptors. *J. Biol. Chem. 280*, 15300−15306.
(33) Ferrari, A., Pellegrini, V., Arcangeli, C., Fittipaldi, A., Giacca, M., and Beltram, F. (2003) Caveolae-mediated internalization of extracellular HIV-1 tat fusion proteins visualized in real time. *Mol. Ther. 8*, 284−294.
(34) Fittipaldi, A., Ferrari, A., Zoppe, M., Arcangeli, C., Pellegrini, V., Beltram, F., and Giacca, M. (2003) Cell membrane lipid rafts mediate caveolar endocytosis of HIV-1 Tat fusion proteins. *J. Biol. Chem. 278*, 34141−34149.
(35) Kaplan, I. M., Wadia, J. S., and Dowdy, S. F. (2005) Cationic TAT peptide transduction domain enters cells by macropinocytosis. *J. Controlled Release 102*, 247−253.
(36) Nakase, I., Tadokoro, A., Kawabata, N., Takeuchi, T., Katoh, H., Hiramoto, K., Negishi, M., Nomizu, M., Sugiura, Y., and Futaki, S. (2007) Interaction of arginine-rich peptides with membrane-associated proteoglycans is crucial for induction of actin organization and macropinocytosis. *Biochemistry 46*, 492−501.
(37) Duchardt, F., Fotin-Mleczek, M., Schwarz, H., Fischer, R., and Brock, R. (2007) A comprehensive model for the cellular uptake of cationic cell-penetrating peptides. *Traffic 8*, 848−866.
(38) Mueller, J., Kretzschmar, I., Volkmer, R., and Boisguerin, P. (2008) Comparison of cellular uptake using 22 CPPs in 4 different cell lines. *Bioconjugate Chem. 19*, 2363−2374.
(39) Maiolo, J. R., Ferrer, M., and Ottinger, E. A. (2005) Effects of cargo molecules on the cellular uptake of arginine-rich cell-penetrating peptides. *Biochim. Biophys. Acta 1712*, 161−172.
(40) El-Sayed, A., Futaki, S., and Harashima, H. (2009) Delivery of macromolecules using arginine-rich cell-penetrating peptides: Ways to overcome endosomal entrapment. *AAPS J. 11*, 13−22.
(41) Varkouhi, A. K., Scholte, M., Storm, G., and Haisma, H. J. (2011) Endosomal escape pathways for delivery of biologicals. *J. Controlled Release 151*, 220−228.
(42) Appelbaum, J. S., LaRochelle, J. R., Smith, B. A., Balkin, D. M., Holub, J. M., and Schepartz, A. (2012) Arginine topology controls escape of minimally cationic proteins from early endosomes to the cytoplasm. *Chem. Biol. 19*, 819−830.
(43) Qian, Z., Liu, T., Liu, Y. Y., Briesewitz, R., Barrios, A. M., Jhiang, S. M., and Pei, D. (2013) Efficient delivery of cyclic peptides into mammalian cells with short sequence motifs. *ACS Chem. Biol. 8*, 423−431.
(44) Lattig-Tunnemann, G., Prinz, M., Hoffmann, D., Behlke, J., Palm-Apergi, C., Morano, I., Herce, H. D., and Cardoso, M. C. (2011) Backbone rigidity and static presentation of guanidinium groups increases cellular uptake of arginine-rich cell-penetrating peptides. *Nat. Commun. 2*, 453.
(45) Mandal, D., Nasrolahi Shirazi, A., and Parang, K. (2011) Cell-penetrating homochiral cyclic peptides as nuclear-targeting molecular transporters. *Angew. Chem., Int. Ed. 50*, 9633−9637.
(46) Zhao, K., Choe, U. J., Kamei, D. T., and Wong, G. C. L. (2012) Enhanced activity of cyclic transporter sequences driven by phase behavior of peptide-lipid complexes. *Soft Matter 8*, 6430−6433.
(47) Lian, W., Upadhyaya, P., Rhodes, C. A., Liu, Y., and Pei, D. (2013) Screening bicyclic peptide libraries for protein-protein interaction inhibitor: Discovery of a tumor necrosis factor-$\alpha$ antagonist. *J. Am. Chem. Soc. 135*, 11990−11995.
(48) Mitra, S., and Barrios, A. M. (2005) Highly sensitive peptide-based probes for protein tyrosine phosphatase activity utilizing a fluorogenic mimic of phosphotyrosine. *Bioorg. Med. Chem. Lett. 15*, 5124−5145.
(49) Stanford, S. M., Panchal, R. G., Walker, L. M., Wu, D. J., Falk, M. D., Mitra, S., Damle, S. S., Ruble, D., Kaltcheva, T., Zhang, S., Zhang, Z. Y., Bavari, S., Barrios, A. M., and Bottini, N. (2012) High-throughput screen using a single-cell tyrosine phosphatase assay reveals biologically active inhibitors of tyrosine phosphatase CD45. *Proc. Natl. Acad. Sci. U.S.A. 109*, 13972−13977.
(50) Yin, J., Straight, P. D., McLoughlin, S. M., Zhou, Z., Lin, A. J., Golan, D. E., Kelleher, N. L., Kolter, R., and Walsh, C. T. (2005) Genetically encoded short peptide tag for versatile protein labeling by Sfp phosphopantetheinyl transferase. *Proc. Natl. Acad. Sci. U.S.A. 102*, 15815−15820.
(51) Holub, J. M., LaRochelle, J. R., Appelbaum, J. S., and Schepartz, A. (2013) Improved assays for determining the cytosolic access of peptides, proteins, and their mimetics. *Biochemistry 52*, 9036−6046.
(52) Huotari, J., and Helenius, A. (2011) Endosome maturation. *EMBO J. 30*, 3481−3500.
(53) Rink, J., Ghigo, E., Kalaidzidis, Y., and Zerial, M. (2005) Rab conversion as a mechanism of progression from early to late endosomes. *Cell 122*, 735−749.
(54) Yu, P., Liu, B., and Kodadek, T. (2005) A high-throughput assay for assessing the cell permeability of combinatorial libraries. *Nat. Biotechnol. 23*, 746−751.
(55) Pratt, W. B., and Toft, D. O. (1997) Steroid receptor interactions with heat shock protein and immunophilin chaperones. *Endocr. Rev. 18*, 306−360.
(56) Picard, D., and Yamamoto, K. R. (1987) Two signals mediate hormone-dependent nuclear localization of the glucocorticoid receptor. *EMBO J. 6*, 3333−3340.
(57) Macia, E., Ehrlich, M., Massol, R., Boucrot, E., Brunner, C., and Kirchhausen, T. (2006) Dynasore, a cell-permeable inhibitor of dynamin. *Dev. Cell 10*, 839−850.
(58) Koivusalo, M., Welch, C., Hayashi, H., Scott, C. C., Kim, M., Alexander, T., Touret, N., Hahn, K. M., and Grinstein, S. (2010) Amiloride inhibits macropinocytosis by lowering submembranous pH and preventing Rac1 and Cdc42 signaling. *J. Cell Biol. 188*, 547−563.
(59) Rodal, S. K., Skretting, G., Garred, O., Vilhardt, F., van Deurs, B., and Sandvig, K. (1999) Extraction of cholesterol with methyl-$\beta$-cyclodextrin perturbs formation of clathrin-coated endocytic vesicles. *Mol. Biol. Cell 10*, 961−974.
(60) Yoshimori, T., Yamamoto, A., Moriyama, Y., Futai, M., and Tashiro, Y. (1991) Bafilomycin A1, a specific inhibitor of vacuolar-type $H^+$-ATPase, inhibits acidification and protein degradation in lysosomes of cultured cells. *J. Biol. Chem. 266*, 17707−17712.
(61) Li, G., D'Souza-Schorey, C., Barbieri, M. A., Roberts, R. L., Klippel, A., Williams, L. T., and Stahl, P. D. (1995) Evidence for phosphatidylinositol 3-kinase as a regulator of endocytosis via activation of Rab5. *Proc. Natl. Acad. Sci. U.S.A. 92*, 10207−10211.
(62) Stenmark, H., Parton, R. G., Steele-Mortimer, O., Lutcke, A., Gruenberg, J., and Zerial, M. (1994) Inhibition of rab5 GTPase activity stimulates membrane fusion in endocytosis. *EMBO J. 13*, 1287−1296.
(63) Rusnati, M., Tulipano, G., Spillmann, D., Tanghetti, E., Oreste, P., Zoppetti, G., Giacca, M., and Presta, M. (1999) Multiple interactions of HIV-1 Tat protein with size-defined heparin oligosaccharides. *J. Biol. Chem. 274*, 28198−28205.
(64) Tyagi, M., Rusnati, M., Presta, M., and Giacca, M. (2001) Internalization of HIV-1 tat requires cell surface heparin sulfate proteoglycans. *J. Biol. Chem. 276*, 3254−3261.
(65) Ziegler, A., and Seelig, J. (2004) Interaction of the protein transduction domain of HIV-1 TAT with heparan sulfate: Binding mechanism and thermodynamic parameters. *Biophys. J. 86*, 254−263.
(66) Goncalves, E., Kitas, E., and Seelig, J. (2005) Binding of oligoarginine to membrane lipids and heparan sulfate: Structural and thermodynamic characterization of a cell-penetrating peptide. *Biochemistry 44*, 2692−2702.
(67) Ziegler, A. (2008) Thermodynamic studies and binding mechanisms of cell-penetrating peptides with lipids and glycosaminoglycans. *Adv. Drug Delivery Rev. 60*, 580−597.
(68) Alonso, A., Sasin, J., Bottini, N., Friedberg, I., Friedberg, I., Osterman, A., Godzik, A., Hunter, T., Dixon, J., and Mustellin, T.

(2004) Protein tyrosine phosphatases in the human genome. *Cell 117*, 699−711.
(69) Driggers, E. M., Hale, S. P., Lee, J., and Terrett, N. K. (2008) The exploration of macrocycles for drug discovery: An underexploited structural class. *Nat. Rev. Drug Discovery 7*, 608−624.
(70) Marsault, E., and Peterson, M. L. (2011) Macrocycles are great cycles: Applications, opportunities, and challenges of synthetic macrocycles in drug discovery. *J. Med. Chem. 54*, 1961−2004.
(71) Liu, T., Qian, Z., Xiao, Q., and Pei, D. (2011) High-throughput screening of one-bead-one-compound libraries: Identification of cyclic peptidyl inhibitors against calcineurin/NFAT interaction. *ACS Comb. Sci. 13*, 537−546.
(72) Dewan, V., Liu, T., Chen, K. M., Qian, Z., Xiao, Y., Kleiman, L., Mahasenan, K. V., Li, C., Matsuo, H., Pei, D., and Musier-Forsyth, K. (2012) Cyclic peptide inhibitors of HIV-1 capsid-human lysyl-tRNA synthetase interaction. *ACS Chem. Biol. 7*, 761−769.
(73) Wu, X., Upadhyaya, P., Villalona-Calero, M. A., Briesewitz, R., and Pei, D. (2013) Inhibition of Ras-effector interactions by cyclic peptides. *Med. Chem. Commun. 4*, 378−382.
(74) Kwon, Y.-U., and Kodadek, T. (2007) Quantative comparison of the telative cell permeability of cyclic and linear peptides. *Chem. Biol. 14*, 671−677.
(75) Rezai, T., Yu, B., Millhauser, G. L., Jacobson, M. P., and Lokey, R. S. (2006) Testing the conformational hypothesis of passive membrane permeability using synthetic cyclic peptide diastereomers. *J. Am. Chem. Soc. 128*, 2510−2511.
(76) Chatterjee, J., Gilon, C., Hoffman, A., and Kessler, H. (2008) N-Methylation of Peptides: A New Perspective in Medicinal Chemistry. *Acc. Chem. Res. 41*, 1331−1342.
(77) Ren, L., Chen, X., Luechapanichkul, R., Selner, N. G., Meyer, T. M., Wavreille, A. S., Chan, R., Iorio, C., Zhou, X., Neel, B. G., and Pei, D. (2011) Substrate specificity of protein tyrosine phosphatases 1B, RPTP$\alpha$, SHP-1, and SHP-2. *Biochemistry 50*, 2339−2356.
(78) LaMontagne, K. R., Jr., Hannon, G., and Tonks, N. K. (1998) Protein tyrosine phosphatase PTP1B suppresses p210 bcr-abl-induced transformation of Rat-1 fibroblasts and promotes differentiation of K562 cells. *Proc. Natl. Acad. Sci. U.S.A. 95*, 14094−14099.
(79) Nguyen, L. T., Chau, J. K., Perry, N. A., de Boer, L., Zaat, S. A. J., and Vogel, H. J. (2010) Serum stabilities of short tryptophan- and arginine-rich antimicrobial peptide analogs. *PLoS One 5*, e12684.